Wake dynamics of external flow past a curved circular cylinder With the free-stream aligned with the plane of curvature

Adelaide de Vecchi, Spencer J. Sherwin, J. Michael R. Graham

Department of Aeronautics, Imperial College, London, SW7 2BT, UK

Abstract. The fundamental mechanism of vortex shedding past a curved cylinder has been investigated at a Reynolds number of 100 using three-dimensional spectral/*hp* computations. Two different configurations are presented herein: in both cases the main component of the geometry is a circular cylinder whose centreline is a quarter of a ring and the inflow direction is parallel to the plane of curvature.
In the first set of simulations the cylinder is forced to transversely oscillate at a fixed amplitude, while the oscillation frequency has been varied around the Strouhal value. Both geometries exhibit in-phase vortex shedding, with the vortex cores bent according to the body's curvature, although the wake topology is markedly different. In particular, the configuration that was found to suppress the vortex shedding in absence of forced motion exhibits now a primary instability in the near wake. A second set of simulations has been performed imposing an oscillatory roll to the curved cylinder, which is forced to rotate transversely around the axis of its bottom section. This case shows entirely different wake features from the previous one: the vortex shedding appears to be out-of-phase along the body's span, with straight cores that tend to twist after being shed and manifest a secondary spanwise instability. Further, the damping effect stemming from the transverse planar motion of the part of the cylinder parallel to the flow is no longer present, leading to a positive energy transfer from the fluid to the structure.

Key words: Vortex shedding, DNS, bluff-bodies, curved cylinder, incompressible flow.

1. Introduction

The intricate dynamics of vortex shedding past curved cylinders is particularly significant for many engineering applications, especially in the offshore industry: the increasing need to exploit deep-water reservoirs has highlighted the lack of a complete insight into the Vortex-Induced Vibrations (VIV) dynamics on long structures such as the marine riser pipes used to convey fluids from the seabed to the sea surface. Steel catenary riser pipes and flexibles are being increasingly used offshore but in spite of their practical importance, curved configurations have received much less attention in the past than straight cylinders.
For a straight circular cylinder the initiation of vortex shedding occurs at a Reynolds number of $47 - 49$. The flow throughout the so called periodic laminar regime, which persists until $Re \approx 180 - 200$, can remain two-dimensional if care is taken to manipulate the body's end conditions such that vortices are shed parallel to the cylinder's axis [10, 21].
Among the first researchers who investigated the effect of curvature on the vortex shedding dynamics at low Reynolds numbers, Takamoto and Izumi [20] reported on

the stable arrangement of vortex rings developed in experiments behind an axisymmetric ring. Leweke and Provansal [15] studied the flow past a ring at sufficiently large aspect ratios (ring perimeter/cross section diameter > 30) that allow approximation of the flow patterns of a straight cylinder by periodic boundary conditions, hence discarding the influence of end effects; with smooth initial conditions parallel vortex shedding was found to be dominant. Their results compare favourably with the numerical simulations of flow past a quarter of ring performed by Miliou et al. [18], who observed in-phase parallel shedding when the flow was directed normal to the plane of curvature.

However only few studies have been carried out with the flow aligned to the plane of curvature. Miliou et al. [17] investigated the same geometries of their previous publication exposed to a constant inflow parallel to the plane of curvature of the quarter ring and observed a fully three-dimensional vortex shedding at $Re = 100$ and $Re = 500$. When the inflow was applied onto the outside surface of the ring the vortex shedding in the upper part of the body was found to drive the wake dynamics in the lower end at one dominant shedding frequency for the whole cylinder's span. In the case of an inflow directed towards the inside of the ring no vortex shedding was detected and the near wake reached a steady state at both Reynolds numbers: in this configuration a drag reduction of 12% was achieved. Miliou et al. related the stabilisation of the wake to the strong velocity component aligned to the cylinder's axis: the shape of the stagnation face in this flow configuration gave rise to an axial flow directed towards the top of the cylinder, where the vortex shedding is expected to occur. This axial flow was associated with the production of streamwise and vertical vorticity components in the top region, which appeared to make the shear layer less susceptible to rolling up in a Von Karman street.

These results can be compared with the outcome of the analysis carried out by Darekar and Sherwin [9] on bodies with a wavy leading edge. The authors observed a variation in the wake width along the span of the wavy cylinder: the flow deflected towards the most downstream section, named "geometrical minimum", generated a wider separated shear layer as compared to the most upstream cross-sections. Different flow regimes could be identified depending on the type of waviness: the so called regime III A was found to suppress vortex shedding with a drag reduction of 16%, leading to a symmetric wake with respect to the cylinder centreline in analogy with the behaviour of the concave configuration investigated by Miliou et al. [17]. The experimental work of Bearman and Owen [4] and Bearman and Tombazis [5] confirms that a sufficiently high wave steepness stabilises the near wake in a time-independent state and results in drag reduction.

In the previous studies on curved and wavy cylinders the body was kept fixed in a constant inflow. In the present work, numerical simulations of forced oscillation cases at $Re = 100$ have been performed on the same geometries investigated in [18] and [17], with the aim to understand the wake dynamics of a highly three-dimensional configuration vibrating inside the the lock-in region: these conditions are meant to capture the fluid dynamic features of a freely vibrating pipe under the simplified assumptions provided by forced oscillations. The potential of the forced oscillation simulations to provide insight into the more complicated dynamics of freely vibrating structures has been the object of many studies on straight cylinders. Varying the amplitude and the frequency of the imposed oscillation Willimason and Roshko [22] compiled a map of the wake patterns induced by body motion and found that not

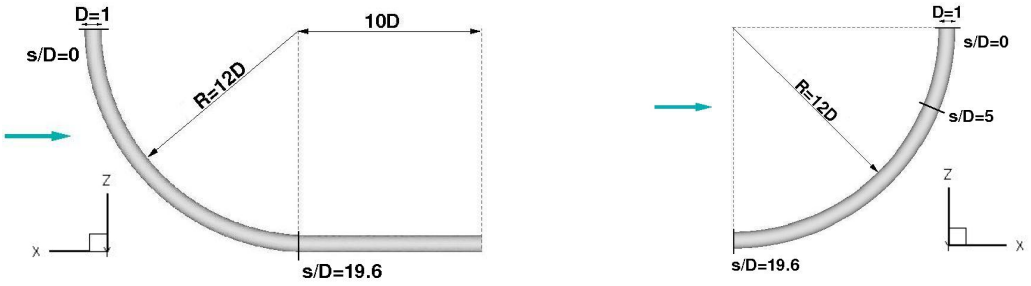

Figure 1. Convex configuration (*left*) and concave configuration (*right*); the arrows indicate the free-stream direction.

all the parameter combinations ensured that the net energy transfer over a cycle was positive, as is required for a body to freely vibrate. More recently, Leontini et al. [14] carried out a numerical study of the parameter space for a two-dimensional cylinder, focussing on the wake modes and energy transfer mechanism; Kalktsis et al. [11] performed a similar investigation showing that qualitative differences in the hydrodynamic forces and wake state occur according to whether the body is forced to vibrate below or above the resonant frequency. Carberry et al. ([8, 7] identified two distinct wake states for a cylinder in forced pure sinusoidal vibration and they could replicate most of the features of a freely oscillating cylinder such as variations of the phase angle and switch in the timing of shedding (see also [16, 6]). However Al Jamal et al. [1] highlighted contrasting results concerning the phase angle variation in forced and free oscillation experiments.

Section 2 presents the geometrical configurations and a brief overview of the computational techniques used in the present work. The results for the convex geometry follow in section 3, focussing on the effect of two different types of motion on the vortex shedding dynamics, while the flow past the concave configuration is presented in section 4. Finally the conclusive remarks are outlined in section 5.

2. Problem description and numerical method

2.1. Geometrical configurations

The computations herein presented involve two types of bodies, sketched in figure 1. According to whether the free-stream is applied on the outside or the inside of the quarter ring two different flow configurations can be identified, named respectively "convex" and "concave". The convex cylinder in figure 1(a) includes a horizontal extension, 10 diameters long, that displaces the outflow plane downstream from the quarter ring in order to allow a full development of the wake; this condition is not necessary in the concave configuration in figure 1(b), which only involves the ring part. A non-dimensional arc length, s/D, has been defined to identify the different spanwise locations: in both cases the end of the ring part is at $s/D = 19.6$ and the top section corresponds to $s/D = 0$.

2.2. Navier-Stokes solver

The three-dimensional computations have been performed using a spectral/*hp* element Navier-Stokes solver developed by Karniadakis and Sherwin [19, 13].
The temporal discretisation is achieved by a stiffy stable splitting scheme which allows the primitive variables to be treated independently over a time step Δt. The solution at time t_{n+1} is obtained from the solution at t_n over three sub-steps. First, the non-linear term is treated explicitly, then a Poisson equation for the pressure is obtained by taking the divergence of the pressure term and by enforcing the incompressibility constraint. Finally the diffusive term is treated implicitly in the last sub-step. Overall one Poisson equation for the pressure and one Helmholtz equation for each of the velocity components are solved for every time step. Further details on the splitting scheme can be found in [13] and [12].

2.3. Numerical boundary conditions

In both configurations the top boundary plane of the computational domain was modelled using a symmetric boundary condition (i.e. $w = 0$, $\frac{du}{dn} \equiv \frac{du}{dz} = 0$ and $\frac{dv}{dn} \equiv \frac{dv}{dz} = 0$), while a fully developed zero stress condition was specified at the outflow. The free-stream velocity was imposed along all other boundaries, with the exception of the inflow in the concave configuration where the cylinder intersects the boundary: here an exponential term was added to the inflow velocity profile to achieve exponential decay within the boundary layer region around the cylinder.

3. Convex configuration

3.1. Forced translation in the transverse direction

In all the simulations performed the amplitude of motion has been kept fixed and equal to $0.5D$, while the input frequencies for the forced oscillation have been varied from $0.9f_s$ to $1.2f_s$, where f_s is the Strouhal frequency for a fixed straight cylinder (see [21]). The values of input frequency and amplitude of oscillation correspond to a point in the parameter plane found by Williamson and Roshko [22] which lies close to the critical curve where the switching from a 2S to a 2P mode of shedding occurs.
The wake topology at $f_i = 1.1f_s$ is displayed in figure 2 (*left*) using λ_2 isosurfaces: the shedding at the top exhibits the features of a 2S mode, with two opposite-signed single vortices shed per oscillation cycle. Due to the three-dimensionality of the model, the vortex cores in the near-wake are bent according to the curvature of the body and start to distort further downstream. In proximity of the horizontal extension they become weaker and deform in a wavy fashion, developing lateral arms of vorticity. Figure 2 (*right*) illustrates the evolution in time of the lift coefficient isocontours in every section perpendicular to the cylinder's axis. The vortex shedding appears to be in phase along the span: considering a fixed time instant in this plot no variation in sign of C_{F_y} occurs as s/D increases. This feature is strictly related to the type of motion and is absent when the body is kept fixed in an uniform flow. In this case Miliou et al. [17] found different shedding dynamics, shown in figure 3a: the vortex cores are straight and their distance from the body's surface changes along the span, as the cylinder is curved. Therefore a gradual phase shift occurs as

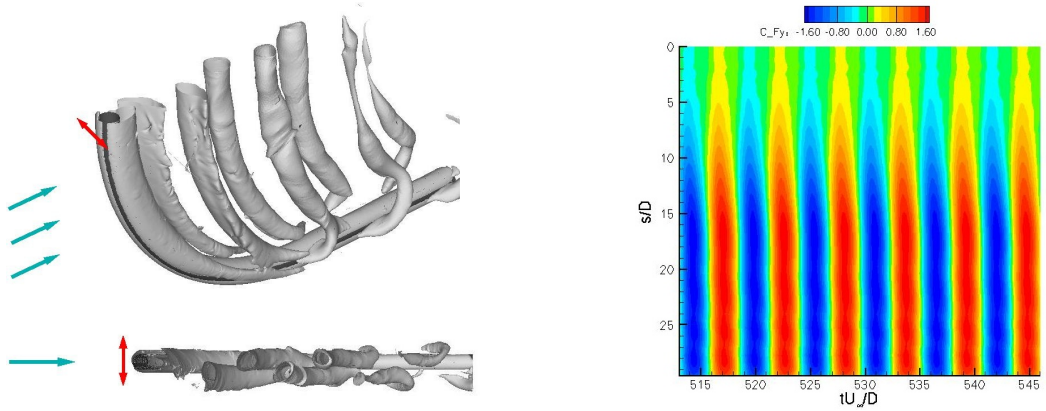

Figure 2. *Left*: Wake topology for the flow past the convex configuration at $f_i = 1.1f_s$ visualised through isosurfaces at $\lambda_2 = -0.1$. *Right*: Time evolution of the sectional lift coefficient along the cylinder's span.

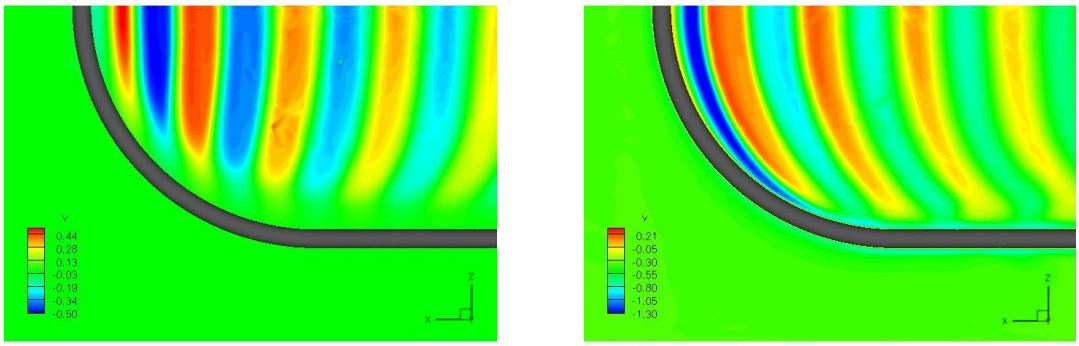

(a) (b)

Figure 3. Isocontours of the v velocity component in the $y-$direction (positive out of paper) at $Re = 100$: (a) Stationary cylinder case. (b) Oscillating cylinder case at $f_i = 1.1f_s$.

a consequence of the delay in the vortex shedding along the span of the cylinder. As expected from theoretical considerations ([3, 2]) if the body oscillates the correlation length of the vortices increases and the coupling of the flow in the spanwise direction becomes stronger, resulting in a more correlated form of shedding (fig. 3b). Further, the distance of the first vortex from the body decreases when the cylinder is forced to oscillate: this is consistent with this case exhibiting higher forces on the body's surface.

The fact that the sectional forces in figure 2 (*right*) do not decrease with increasing s/D may appear in contrast to the weakening of the shedding in the lower part of the cylinder shown in figure 2 (*left*): however, in the horizontal extension ($s/D > 19.6$) the body undergoes only a drag type force in the y-direction due to the cross flow, since the inflow is parallel to the cylinder's axis and does not generate vortex shedding. Therefore the horizontal part behaves like a slender body and provides a strong hydrodynamic damping to the whole structure. In figure 6 the time-averaged components of the lift coefficient in phase with the velocity, CL_v, and with the

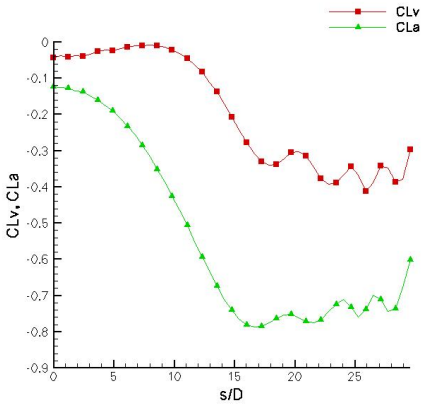

Figure 4. Spanwise distribution of the time-averaged lift coefficient components in phase with the velocity (CL_v) and with the acceleration (CL_a).

acceleration, CL_a, are plotted against the non-dimensional arc-length. CL_v, which predicts when free vibration should take place, reaches the most negative value for $s/D > 20$ and increases towards the top sections: therefore the net energy per cycle is negative, as opposed to flow-induced motions which require positive energy transfer from the fluid to the cylinder.
The wake topology at the other frequencies tested is substantially similar to the one presented above and a 2S type of shedding is observed in all cases. As expected from the theory, the formation length is found to decrease with increasing shedding frequency, resulting in higher forces on the cylinder's surface. However these flow states lie outside the region of positive energy transfer and therefore predict that free vibrations would in fact not occur, in contrast to the results obtained for a straight cylinder with the same input parameters.

3.2. Forced rotation about the horizontal extension axis

As shown in the previous simulations, the lower part of the body acts like a strong hydrodynamic damper in forced translation, preventing the whole structure from being excited by the flow. To avoid this mechanism an oscillatory roll motion about a horizontal extension axis through the lower part of the cylinder has been imposed as an alternative: the maximum amplitude, equal to $0.5D$, is thus reached at the top section and linearly decreases with decreasing distance to the roll axis.
At an input frequency equal to $f_i = 0.9f_s$, the λ_2 isosurfaces in figure 5 (*left*) show that the shed cores twist around their axes and exhibit spanwise waviness. Furthermore they are only slightly bent according to the cylinder's curvature and detach from the main vortex at different spanwise locations for every time instant: the imposed motion leads to out of phase shedding and thus to the non uniform spanwise distribution of the sectional lift coefficient illustrated in figure 5 (*right*). In contrast to the translational motion previously considered, the main vortex is weaker and does not envelope the horizontal extension, which is now fixed. In fig. 6 the time-averaged components of the lift coefficient in phase with the velocity reach positive values for $2 < s/D < 12$: in this interval the energy is conveyed from the fluid to the structure, which is subsequently excited (phase angle $\phi \in [0, 180°]$). Therefore

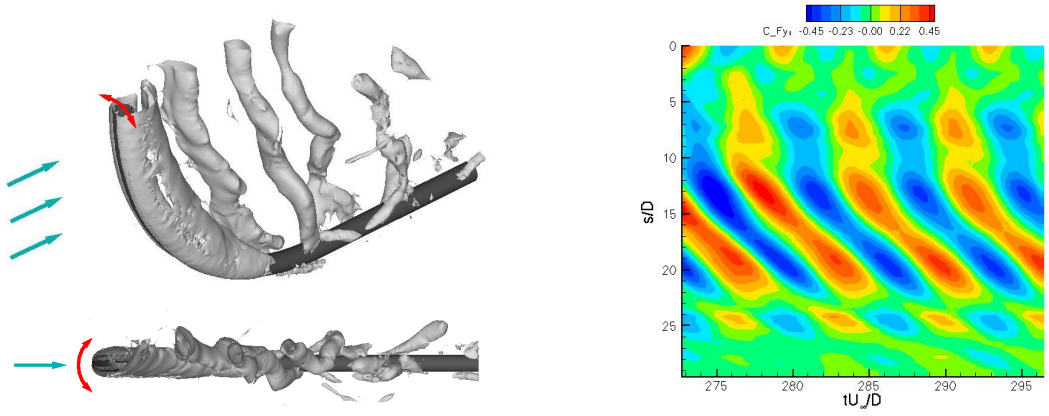

Figure 5. Left: Wake topology for the flow past the convex configuration at $f_i = 0.9f_s$ visualised through isosurfaces at $\lambda_2 = -0.1$. *Right*: Time evolution of the sectional lift coefficient along the cylinder's span.

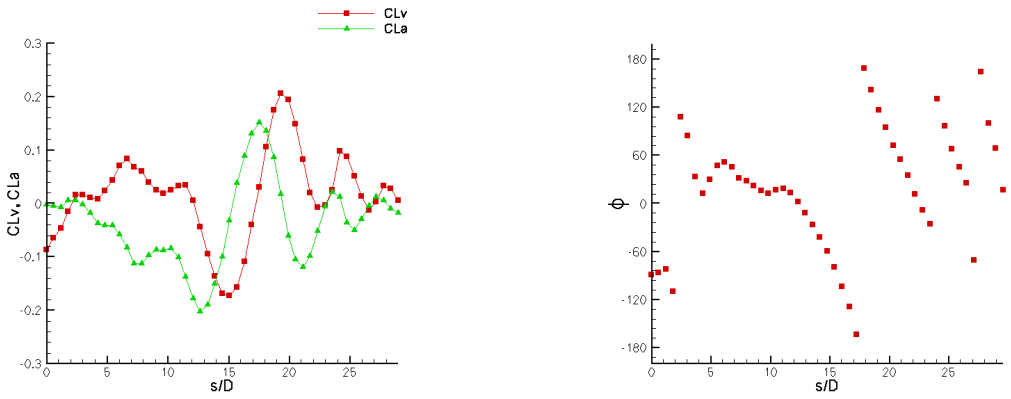

Figure 6. Spanwise distribution of the time-averaged lift coefficient components in phase with the velocity, CL_v, and with the acceleration, CL_a (*left*) and of the phase angle ϕ (*right*).

the damping effect stemming from the lower part of the body is inhibited and the resulting energy transfer for the entire structure is positive.

4. Concave configuration

Three-dimensional DNS of forced oscillation has been performed on the second configuration of figure 1 using the same input parameters as the convex case simulations. The vortices in the wake of the concave cylinder are visualised in figure 7 (*left*) through λ_2 isosurfaces. As the free-stream velocity is now directed towards the inside of the curved cylinder, the vortex cores are not interacting with the structure when they are convected downstream; however they appear to be bent according to the curvature of the leading edge in this case as well. Figure 7 illustrates for comparison the wake past a fixed cylinder in an uniform flow at the same Reynolds

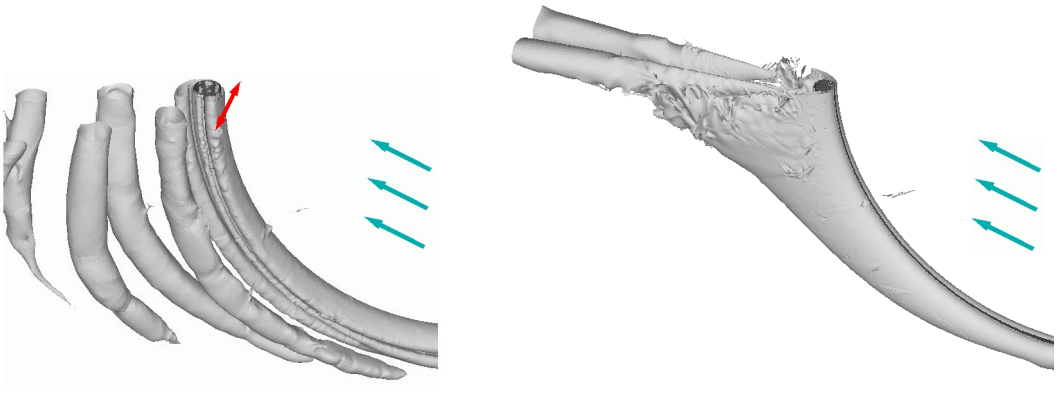

Figure 7. Comparison of the wake topology for the flow past the concave configuration. *Left*: forced oscillation at $f_i = 1.1f_s$, isosurfaces at $\lambda_2 = -0.1$. *Right*: steady wake in the stationary case visualised at $\lambda_2 = -0.01$ (Miliou et al. [17]).

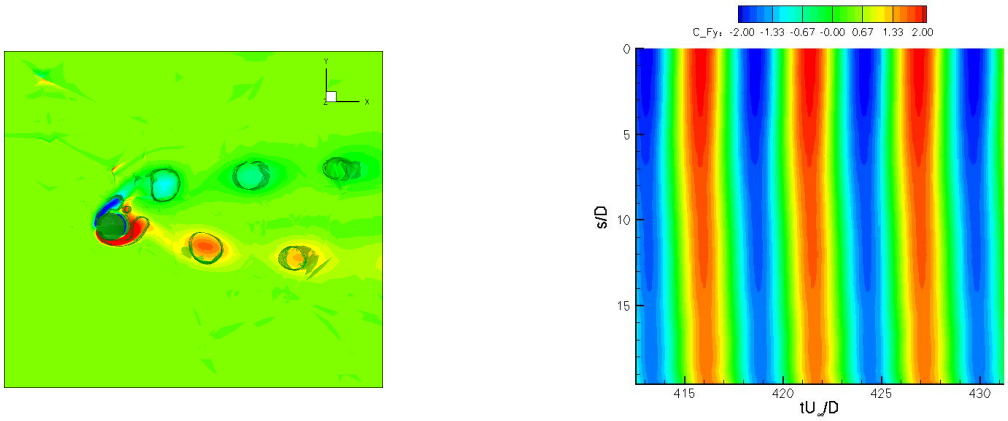

Figure 8. Left: Spanwise vorticity isocontours overlaid on $\lambda_2 = -0.1$ isosurfaces in the case of forced translation (concave configuration). *Right*: Time evolution of the sectional lift coefficient along the cylinder's span.

number [17, 18]. This case was found to suppress vortex shedding, giving rise to a steady wake without interaction between the shear layers. Moreover, in the absence of motion a variation of the wake width along the span was observed: the top section exhibited the widest wake, while the bottom one the narrowest. This phenomenon was related to the strong component of axial flow stemming from the stagnation face curvature and to the associated production of vorticity in the x- and y- direction in the developing shear layers at the top of the cylinder. As shown in figure 7 (*left*) and 8 (*left*), the transverse motion results in a disruption of this stabilising mechanism: the axial flow direction is not constant along the span and the formation of vorticity in the part of the cylinder most susceptible to periodic vortex shedding is weakened. The near-wake topology appears to be completely different from the one obtained for the convex configuration at the same input frequency. Figure 8 (*left*) shows that the shear layers are more contracted, generating higher forces on the body. Further, both the near and far wakes are much wider than in the convex configuration shown

in figure 2 (*left*). This can be related to the induced velocity stemming from the circulation in the curved cores that is now directed towards the outside of the wake and not towards the centre-line as in the convex case. The secondary core between the shear layers is generated from the vorticity in the base region, which separates under the effect of motion; during one half cycle the strength of this vortex decreases until it fades out before reforming from the opposite-signed base vorticity in the remaining half of the motion.
Finally we note that the absence of the horizontal extension allows the surface forces to decrease towards the lower part of the body, where the shedding is less strong. Figure 8 (*right*) shows that the shedding is in-phase along the whole length of the body and there is no switching in time.

5. Concluding remarks

The vortex shedding past two different curved configurations has been investigated by imposing a sinusoidal motion on the body. In particular we have addressed the question of the role played in the near-wake dynamics by the orientation of the stagnation face and of the effect of two different types of forced oscillation on the forces distribution and energy transfer.
In the convex configuration case the forced translation has led to in-phase shedding, with bent vortex cores that detach from the shear layers at the same time for every spanwise location. The strong spanwise correlation induced by the motion prevails on the effect of curvature that was responsible for the phase shift when the body was stationary. However the influence of curvature in forced vibration is significant in the lower region, where the cylinder is aligned with the inflow direction: the horizontal extension behaves in fact like a transversely oscillating slender body, causing a high hydrodynamic damping which ultimately results in a negative energy transfer.
To replicate the features of a freely oscillating configuration, a transverse rotation about the horizontal extension has been imposed on this geometry: the amplitude of oscillation linearly decreases along the span, while the frequency is fixed. This kind of motion allows the body to be excited by the fluid, without the damping effect stemming from the horizontal extension motion. The wake topology results markedly different from the case of forced translation and exhibits straight vortex cores and out-of-phase shedding.
Finally the effect of forced transverse vibration has been investigated in the concave configuration. In the absence of motion this geometry was found to suppress vortex shedding; the controlled oscillation disrupts the stabilising mechanism triggered by curvature and gives rise to a wide wake with staggered arrays of vortices shed alternately from the sides of the cylinder.
The present work highlights the lack of a full correspondence between the flow states observed in forced oscillations for curved and straight cylinders; this suggests that a redefinition of the lock-in boundaries for more complex geometries should be undertaken in order to understand the combined influence of motion and curvature on the vortex shedding.

References

[1] H. Al Jamal and C. Dalton. The contrast in phase angles between forced and self-excited oscillations of a circular cylinde. *Journal of Fluid and Structures*, 20:467–482, 2005.

[2] P.W. Bearman. Vortex shedding from oscillating bluff bodies. *Annual Review of Fluid Mechanics*, 16:195–222, 1984.

[3] P.W. Bearman and E.D Obasaju. An experimental study of pressure fluctuations on fixed and oscillating square-section cylinders. *Journal of Fluid Mechanics*, 119:297–321, 1982.

[4] P.W. Bearman and J.C. Owen. Reduction of bluff-body drag and suppression of vortex shedding by the introduction of wavy separation lines. *Journal of Fluid and Structures*, 12:123–130, 1998.

[5] P.W. Bearman and N. Tombazis. A study of the three-dimesional aspects of vortex shedding from a bluff body with a mild geometric disturbance. *Journal of Fluid Mechanics*, 330:85–112, 1997.

[6] H.M. Blackburn and R.D. Henderson. A study of two-dimensional flow past an oscillating cylinder. *Journal of Fluid Mechanics*, 385:255–286, 1999.

[7] J. Carberry, R. Govardhan, J. Sheridan, D. Rockwell, and C.H.K. Williamson. Wake states and response branches of forced and freely oscillating cylinders. *European Journal of Mechanics, B*, 23:89–97, 2004.

[8] J. Carberry, J. Sheridan, and D. Rockwell. Controlled oscillations of a cylinder: forces and wake modes. *Journal of Fluid Mechanics*, 538:31–69, 2005.

[9] R. M. Darekar and S. J. Sherwin. Flow past a square-section cylinder with a wavy stagnation face. *Journal of Fluid Mechanics*, 426:263–295, 2001.

[10] H. Eisenlohr and H. Ecklemann. Vortex splitting and its consequences in the vortex street wake of cylinders at low reynolds number. *Physics of Fluids*, A1:189–192, 1989.

[11] L. Kalktsis, G.S. Triantafyllou, and M. Ozbas. Excitation, inertia, and drag forces on a cylinder vibrating transversely to a steady flow. *Journal of Fluid and Structures*, 23:1–21, 2007.

[12] G. E. Karniadakis, M. Israeli, and S. A. Orszag. High-order splitting methods for the incompressible navier-stokes equations. *Journal of Computational Physics*, 97:414–443, 1991.

[13] G. E. Karniadakis and S. J. Sherwin. *Spectral/hp Element Methods for CFD*. Oxford University Press, 2005.

[14] J.S. Leontini, B.E. Stewart, M.C. Thompson, and K. Hourigan. Wake state and energy transitions of an oscillating cylinder at low reynolds number. *Physics of Fluids*, 18, 2006.

[15] T. Leweke and M. Provansal. The flow behind rings - bluff-body wakes without end effects. *Journal of Fluid Mechanics*, 288:265–310, 1995.

[16] J.R. Meneghini and P.W. Bearman. Numerical simulations of high amplitude oscillatory flow about a circular cylinder. *Journal of Fluids and Structures*, 9:435–455, 1995.

[17] A. Miliou, A. de Vecchi, S. J. Sherwin, and J. M. R. Graham. Wake dynamics of external flow past a curved cylinder with the free-stream aligned to the plane of curvature. *Under consideration for publication in Journal of Fluid Mechanics*.

[18] A. Miliou, S.J. Sherwin, and J.M.R. Graham. Fluid dynamic loading on curved riser pipes. *ASME Journal of Offshore Mechanics and Arctic Engineering*, 125:176–182, 2003.

[19] S.J. Sherwin and G.E. Karniadakis. Tetrahedral hp finite elements: algorithms and flow simulations. *Journal of Computational Physics*, 124:14–45, 1996.

[20] M. Takamoto and K. Izumi. Experimental observation of stable arrangement of vortex rings. *Physics of Fluids*, 24:1582–1583, 1981.

[21] C.H.K. Williamson. Vortex shedding in the wake of a circular cylinder at low reynolds numbers. *Journal of Fluid Mechanics*, 206:579–627, 1989.

[22] C.H.K. Williamson and A. Roshko. Vortex formation in the near wake of an oscillating cylinder. *Journal of Fluid and Structures*, 2:355–381, 1988.